combustible mixture during the process. After 10°AC BTDC, there is a significant increase of OH and H radicals with the increase of EFHB. Meanwhile, the crank angle corresponding to the peak mass of these radicals is advanced and the gasoline consumption rate becomes faster. This is because PHG can accelerate the reaction rate of $OH+H_2 \Leftrightarrow H_2O+H$ and generate more H radicals, which in turn promotes the reaction rate of $H+O_2 \Leftrightarrow OH+O$ [16]. As important branched reactions in gasoline combustion process, these two reactions promote each other and directly determine the burning rate of the fuel. All in all, PHG can increase the mass of OH, O and H radicals and effectively shorten the formation process of fire nuclei. What's more, it has an accelerating effect on the burning rate of fuel and can increase the rate of gasoline consumption. Namely, PHG is beneficial to the improvement of fuel utilization rate of XRE.

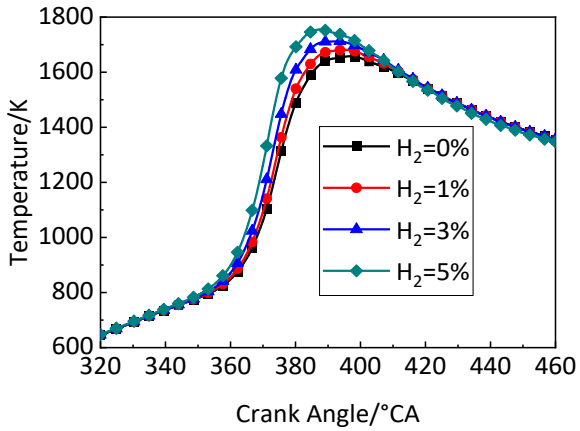

Fig. 7. In-cylinder mean temperature versus crank angle under different EFHB

In order to compare the difference of in-cylinder combustion between PHG and pure gasoline, the variation curves of in-cylinder mean temperature versus crank angle under different EFHB are presented in Fig. 7. It is found that PHG can significantly increase mean temperature of the combustion chamber. Meanwhile, the crank angle corresponding to the peak temperature is advanced. As the EFHB increases, the peak temperature also increases. When the EFHB is 5%, the peak temperature in the combustion chamber is increased by 6.4% compared with pure gasoline.

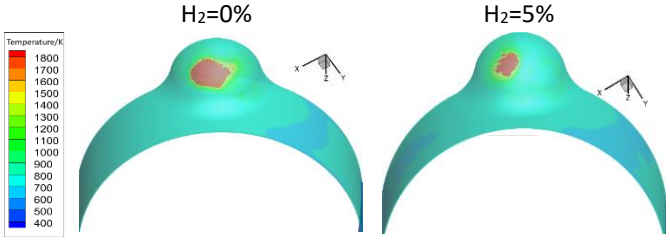

5°CA ATDC

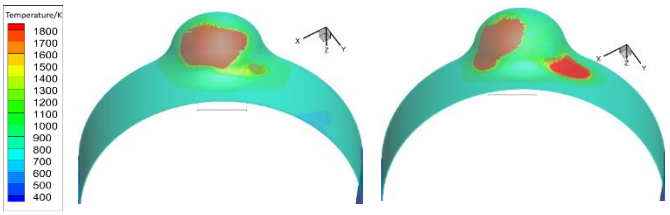

10°CA ATDC

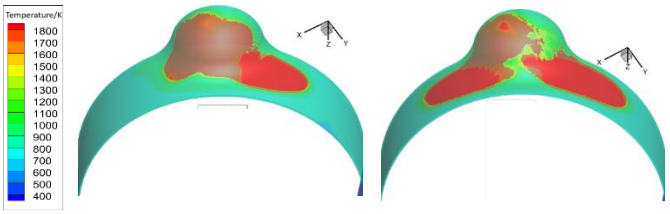

15°CA ATDC

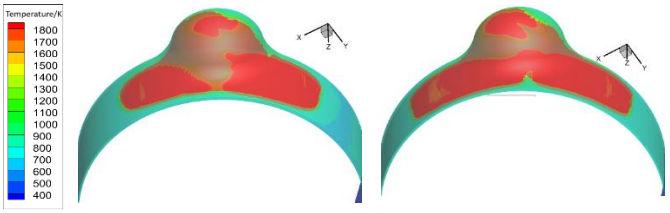

20°CA ATDC

Fig. 8. Cloud map of in-cylinder temperature change

Fig. 8 displays the comparison of the in-cylinder temperature clouds for pure gasoline and PHG at 5% EFHB for four moments. At 5°CA ATDC, the difference between the two temperature clouds is not significant. The combustion area of pure gasoline is located in the middle of the spherical combustion chamber while that of PHG is on the left side of the combustion chamber. At 10°CA ATDC, the difference between the two temperature clouds begins to appear. The combustion area of pure gasoline continues to expand in the middle of the chamber. The combustion area of PHG not only expands on the left side of the combustion chamber, but also on the right side of the chamber. At 15°CA ATDC, the combustion area of pure gasoline spreads to the right side of the chamber. By comparison, the combustion area of PHG expands on the left and right sides respectively. At 20°CA ATDC, the temperature cloud distribution of both tends to be the same. But the combustion area of PHG is larger than that of pure gasoline. Moreover, the flame center temperature is higher than that of pure gasoline.

From the above, it can be seen that the combustion of HB mixture on the left and right sides of the combustion chamber is obviously better than that of pure gasoline. Namely, the flame propagation speed to the left and right sides of the combustion chamber is obviously greater than that of pure gasoline. These indicate that blending a small amount of hydrogen can make the flame propagate farther and improve the combustion of fuel on the left and right sides of the

combustion chamber. Besides, the PHG can make the combustion area more uniform and help solve the problem of incomplete combustion in the slit on both sides.

4. CONCLUSIONS

In this paper, a 3D numerical simulation model of an XRE with PHG is established, and the engine flow filed and combustion performances are studied under different EFHB. The following conclusions are obtained:

(1) Two vortexes in opposite directions are generated on both sides of the combustion chamber in the intake stage. They interact with each other and promote the mixing process of gas components, leading to the maximum of in-cylinder mean TKE and vorticity.

(2) In respect to the combustion performance of XRE, the PHG can increase the content of OH, H and O radicals, and promote the generation of radicals, leading to the acceleration of the consumption rate of gasoline. The mixing of hydrogen in XRE could accelerate the combustion speed, and widen the flame to both sides of the combustion chamber, and present a more uniform combustion area.

ACKNOWLEDGEMENT

Thanks for the support from the Science and Technology on Plasma Dynamics Laboratory Program (No.6142202210201) and The Green Aerotechnics Research Institute of Chongqing Jiaotong University.

REFERENCE

[1] Shkolnik A, Littera D, Nickerson M, et al. Development of a small rotary SI/CI combustion engine[C]. SAE Technical Paper, 2014.

[2] Yang J, Ji C, Wang S, et al. Numerical investigation on the mixture formation and combustion processes of a gasoline rotary engine with direct injected hydrogen enrichment [J]. Applied Energy, 2018, 224: 34-41.

[3] Amrouche F, Erickson P, Park J. Extending the lean operation limit of a gasoline Wankel rotary engine using hydrogen enrichment[J]. International Journal of Hydrogen Energy. 2016, 41(32):14261-14271.

[4] Nickerson M, Kopache A, Shkolnik A, et al. Preliminary development of a 30 kW heavy fueled compression ignition rotary X engine with target 45% brake thermal efficiency[C]. SAE Technical Paper, 2018.

[5] Costa T, Nickerson M, Littera D, Martins J, et al. Measurement and prediction of heat transfer losses on the XMv3 rotary engine[J]. SAE Int. J. Engines, 2016, 9(4):2368-2380.

[6] Littera D, Nickerson M, Kopache A, et al. Development of the XMv3 high efficiency cycloidal engine[C]. SAE Technical Paper, 2015.

[7] Leboeuf M, Dufault J, Nickerson M, et al. Performance of a low-blowby sealing system for a high efficiency rotary engine[C]. SAE Technical Paper, 2018.

[8] Wang S, Ji C, Zhang B, et al. Effect of CO2 dilution on combustion and emissions characteristics of the hydrogen-enriched gasoline engine[J]. Energy, 2016, 96:118-126.

[9] Ji C, Cong X, Wang S, et al. Performance of a hydrogen-blended gasoline direct injection engine under various second gasoline direct injection timings[J]. Energy Conversion and Management, 2018, 171:1704-1711.

[10] Fan B, Zhang Y, Pan J, et al. The influence of hydrogen injection strategy on mixture formation and combustion process in a port injection rotary engine fueled with natural gas/hydrogen blends[J]. Energy Conversion and Management, 2018, 173:527-538.

[11] Fan B, Pan J, Liu Y, et al. Numerical investigation of mixture formation and combustion in a hydrogen direct injection plus natural gas port injection rotary engine[J]. International Journal of Hydrogen Energy, 2018, 43:4632-4644.

[12] Yang J, Ji C, Wang S, et al. Numerical investigation of the effects of hydrogen enrichment on combustion and emissions formation processes in a gasoline rotary engine [J]. Energy Conversion and Management, 2017, 151: 136-146.

[13] Liu Y, Jia M, Xie M, et al. Enhancement on a skeletal kinetic model for primary reference fuel oxidation by using a semidecoupling methodology[J]. Energy & Fuels, 2012, 26:7069-7083.

[14] Yang J, Ji C, Wang S, et al. A comparative study of mixture formation and combustion processes in a gasoline Wankel rotary engine with hydrogen port and direct injection enrichment [J]. Energy conversion and management, 2018, 168: 21-31.

[15] Su T, Ji C, Wang S, et al. Investigation on combustion and emissions characteristics of a hydrogen-blended n-butanol rotary engine [J]. International Journal of Hydrogen Energy, 2017, 42(41): 26142-26151.

[16] Ji C, Su T, Wang S, et al. Effect of hydrogen addition on combustion and emissions performance of a gasoline rotary engine at part load and stoichiometric conditions[J]. Energy conversion and management, 2016, 121: 272-280.